GluN2B subunit deletion reveals key role in acute and chronic ethanol sensitivity of glutamate synapses in bed nucleus of the stria terminalis

Tiffany A. Wills[a], Jason R. Klug[b,c,1], Yuval Silberman[a,1], Anthony J. Baucum[a], Carl Weitlauf[b], Roger J. Colbran[a,b,c,d], Eric Delpire[a,b,c,d], and Danny G. Winder[a,b,c,d,2]

[a]Department of Molecular Physiology and Biophysics, [b]Center for Molecular Neuroscience, [c]Vanderbilt Brain Institute, and [d]J. F. Kennedy Center for Research on Human Development, Vanderbilt University School of Medicine, Nashville TN 37232-0615

Edited by Robert C. Malenka, Stanford University School of Medicine, Stanford, CA, and approved December 13, 2011 (received for review August 23, 2011)

The bed nucleus of the stria terminalis (BNST) is a critical region for alcohol/drug-induced negative affect and stress-induced reinstatement. NMDA receptor (NMDAR)-dependent plasticity, such as long-term potentiation (LTP), has been postulated to play key roles in alcohol and drug addiction; yet, to date, little is understood regarding the mechanisms underlying LTP of the BNST, or its regulation by ethanol. Acute and chronic exposure to ethanol modulates glutamate transmission via actions on NMDARs. Despite intense investigation, tests of subunit specificity of ethanol actions on NMDARs using pharmacological approaches have produced mixed results. Thus, we use a conditional GluN2B KO mouse line to assess both basal and ethanol-dependent function of this subunit at glutamate synapses in the BNST. Deletion of GluN2B eliminated LTP, as well as actions of ethanol on NMDAR function. Further, we show that chronic ethanol exposure enhances LTP formation in the BNST. Using KO-validated pharmacological approaches with Ro25-6981 and memantine, we provide evidence suggesting that chronic ethanol exposure enhances LTP in the BNST via paradoxical extrasynaptic NMDAR involvement. These findings demonstrate that GluN2B is a key point of regulation for ethanol's actions and suggest a unique role of extrasynaptic GluN2B-containing receptors in facilitating LTP.

extended amygdala | synaptic plasticity | excitatory transmission

The bed nucleus of the stria terminalis (BNST) is an area of the brain that underlies the negative reinforcing properties associated with drug/alcohol dependence, and has been shown in numerous studies to be critical for expression of stress-induced reinstatement of drug-seeking behavior (1–7). Although the molecular and physiological regulation of drug-related behaviors is not completely understood, numerous studies suggest a key role for synaptic plasticity in the long-term actions of alcohol and drugs of abuse. Thus, understanding how plasticity is regulated by ethanol and drugs of abuse in the BNST will be vital to the therapeutic development of treatments for alcohol and drug use disorders.

A primary action of ethanol is inhibition of NMDA receptor (NMDAR) function (8–10). The NMDAR is a heterotetrameric complex composed of two obligatory GluN1 (formerly NR1) subunits and two GluN2 (formerly NR2) and/or GluN3 subunits (11). Numerous subunit combinations are possible, with eight different splice variants of GluN1 subunit and four distinct GluN2 subunit isoforms (A, B, C, and D). The predominant GluN2 subunits in adult forebrain are GluN2A and GluN2B, which dictate many channel properties, such as decay time, localization, intracellular signaling, and conductance (11, 12).

Exact mechanisms by which ethanol inhibits NMDAR function are not well-defined but fall into two categories: one involving direct interactions of ethanol with the NMDAR and/or the NMDAR–membrane interface, and another involving ethanol-driven posttranslational modifications of the NMDAR (13–17). It remains unclear whether there is subunit selectivity (GluN2A vs. GluN2B) for these acute ethanol effects in vivo. Many studies have pharmacologically addressed this question and yielded mixed results (18–23). In the BNST, ethanol dose-dependently inhibits NMDARs, and this effect is attenuated with a GluN2B antagonist (24, 25). More chronic ethanol treatments have been shown to alter NMDAR expression, signaling, and plasticity during withdrawal (26, 27) in portions of the BNST. Indeed, in many brain regions, withdrawal from chronic ethanol increases GluN2B expression (28–33). This enhancement could be produced by increased expression in synaptic or extrasynaptic populations of GluN2B-containing NMDARs (34, 35). A recent report suggests that ethanol withdrawal produces lateral movement of synaptic GluN2B populations to extrasynaptic sites in hippocampal neurons, perhaps facilitating future plasticity (35).

Delineation of roles of GluN2A and GluN2B has met with difficulties because of problems with nonselective drugs (36–39) and lethality of constitutive KOs (40). The current work set out to determine the role of GluN2B in actions of acute and chronic ethanol on glutamate synapses in dorsal lateral (dl) BNST using a GluN2B conditional KO line. Results from these studies demonstrate a key role for GluN2B in both the acute and chronic actions of ethanol. Moreover, a combination of genetic and pharmacological approaches suggests an unanticipated role of extrasynaptic receptors in positively modulating long-term potentiation (LTP) in the BNST after chronic ethanol exposure.

Results

Validation of GluN2B Deletion. Western blot analysis of punches from isolated dlBNST showed dramatically reduced GluN2B levels [21% ± 4% of control; $t(14) = 10.62$; $P < 0.0001$; Fig. 1*B*], similar to other results obtained with this mouse model (41). Furthermore, there was a significant decrease in decay time of evoked NMDAR excitatory postsynaptic currents (EPSCs) in BNST neurons from KO mice [control: 390.9 ± 70.0 ms vs. GluN2B KO: 164.9 ± 53.0 ms; $t(15) = 2.622$; $P < 0.05$; Fig. 1*C*], consistent with previous studies using GluN2B KO mice to examine hippocampal excitatory transmission (7, 42).

Basal Glutamate Transmission in GluN2B KO Mice. To begin to assess the impact of GluN2B deletion on glutamatergic synapses, we probed levels of other NMDAR subunits and associated proteins. As has been observed in other GluN2B KO mice (7, 41), GluN1 levels were reduced [34 ± 4% of controls; $t(14) = 9.42$; $P <$

Author contributions: T.A.W. and D.G.W. designed research; T.A.W., J.R.K., Y.S., A.J.B., and C.W. performed research; R.J.C. and E.D. contributed new reagents/analytic tools; T.A.W., J.R.K., Y.S., A.J.B., and C.W. analyzed data; and T.A.W., R.J.C., and D.G.W. wrote the paper.

The authors declare no conflict of interest.

This article is a PNAS Direct Submission.

[1]J.R.K. and Y.S. contributed equally to this work.

[2]To whom correspondence should be addressed. E-mail: danny.winder@vanderbilt.edu.

See Author Summary on page 1376.

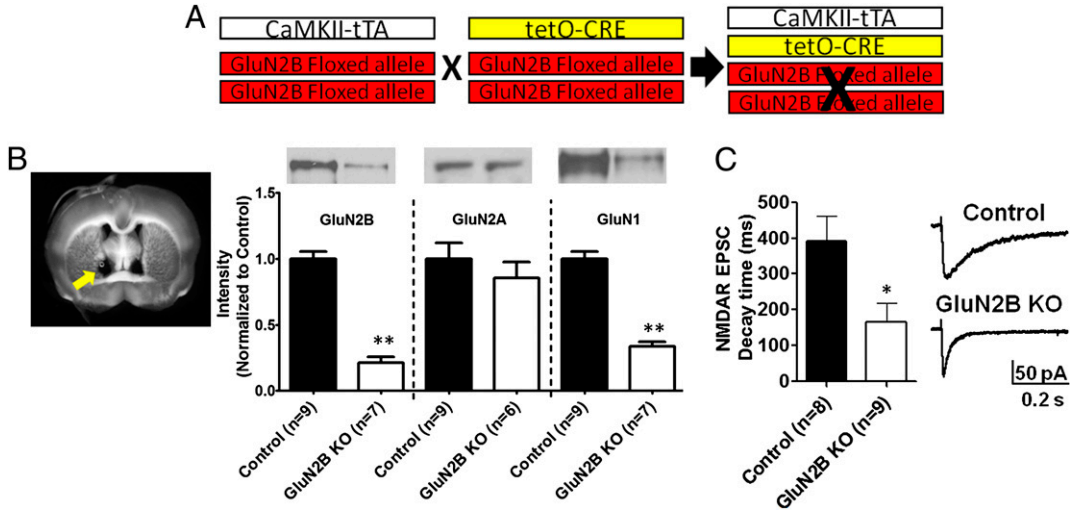

Fig. 1. Breeding strategy and verification of GluN2B KO mice. (*A*) Schematic of breeding strategy for production of GluN2B KO mice. Mice are homozygous for the GluN2Bfl/fl allele and heterozygous for either the CaMKIIα-tTA transgene or tetO-CRE transgene. (*B*) Western blot analysis of GluN2B, GluN1, and GluN2A expression levels in dlBNST (representative image of punch locations marked with yellow arrow) of control (single-transgene and WT littermates) and GluN2B KO mice. (*C*) (*Left*) Decay time of evoked NMDAR EPSCs in neurons from control and GluN2B KO mice. (*Right*) Representative traces of NMDAR EPSCs from control and GluN2B KO mice. $*P < 0.05$; $**P < 0.01$.

0.0001; Fig. 1*B*], whereas levels of GluN2A remained unchanged [85.4 ± 12% of controls; $t(13) = 0.8179$; P = not significant (N.S.); Fig. 1*B*]. There was also a reduction in CaMKIIβ [69.4 ± 8% of controls; $t(14) = 4.411$; $P < 0.001$], a nonsignificant trend for reduced CaMKIIα [69.3 ± 13% of controls; $t(14) = 1.926$; $P = 0.075$], and normal levels of GluA1 [79 ± 13% of controls; $t(14) = 1.37$; P = N.S.].

We next assessed basal excitatory transmission onto dlBNST neurons using whole-cell patch-clamp recordings. AMPA receptor (AMPAR)-mediated spontaneous EPSC (sEPSC) amplitude was unchanged by GluN2B deletion [$t(11) = 1.443$; P = N.S.; Fig. 2*A*]; however, there was a significant increase in sEPSC frequency [$t(11) = 2.334$; $P < 0.05$; Fig. 2*A*]. Consistent with these data, paired pulse ratios (PPRs) of evoked AMPAR-mediated EPSCs were reduced over all interstimulus intervals (20, 40, and 60 ms) in GluN2B KO mice compared with controls [$F(1,36) = 5.95$; $P < 0.05$; Fig. 2*B*]. Together, these data indicate that glutamate release probability is increased in dlBNST of GluN2B KO mice.

We also examined the ratios of evoked EPSCs at different holding potentials to generate an AMPA/NMDA ratio. Consistent with a previous study using a GluN2B KO to study excitatory transmission in the hippocampus (42), AMPA/NMDA ratios of evoked EPSCs recorded from GluN2B KO mice were substantially increased relative to controls [$t(10) = 4.113$; $P < 0.005$; Fig. 2*C*]. This could be a function of either enhanced AMPAR function, reduced functional NMDAR contribution at the synapse, or a combination of the two. Because GluA1 protein levels and sEPSC amplitudes are unchanged in GluN2B KO mice, these data are consistent with reduced function of NMDARs.

GluN2B Is Necessary for LTP in dlBNST. We next assessed the role of GluN2B in BNST LTP induction using both the GluN2B KO as well as the GluN2B antagonist Ro25-6981. We previously reported

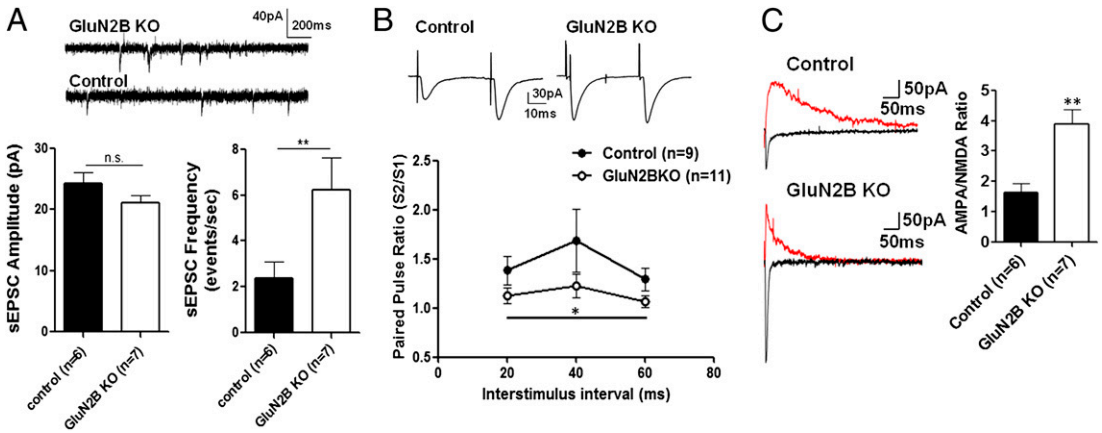

Fig. 2. Basal glutamate transmission in GluN2B KO mice. (*A*) Representative traces of sEPSCs from GluN2B KO mice and controls. Quantification of sEPSC amplitude and frequency in dlBNST neurons from control (single-transgene and WT littermates) and GluN2B KO mice is shown. (*B*) Representative traces of paired EPSCs at the 40-ms interstimulus interval in control and GLuN2B KO mice. PPRs of evoked 100- to 200-pA responses elicited with stimulus intervals of 20, 40, and 60 ms in dlBNST neurons from control (single-transgene and WT littermates) and GluN2B KO mice are plotted. (*C*) Representative traces at +40 mV (red) and −70 mV (black) in neurons from control and GluN2B KO mice. Estimated AMPA/NMDA ratios were obtained from evoked EPSCs, comparing peak current recorded at −70 mV (AMPAR component) with current measured at +40 mV at 50 ms (predominantly NMDAR component). $*P < 0.05$; $**P < 0.01$.

that LTP in the BNST was intact in slices obtained from GluN2A KO mice (39). In contrast, tetanization failed to produce LTP in dlBNST from slices obtained from GluN2B KO mice (Fig. 3*A*). There was a significant difference during the first 10 min following tetanus between GluN2B KO mice and controls [$t(26) = 2.295$; $P < 0.05$], with field potentials from GluN2B KO mice returning to baseline more quickly than controls. This difference between groups was maintained at later time points, with GluN2B KO field potentials returning to pretetanus levels [$t(26) = 2.878$; $P < 0.01$; 51–60 min after tetanus]. It is possible that the loss of LTP in these experiments does not specifically reflect the loss of GluN2B but rather a generalized reduction of NMDAR function. To address this issue, we repeated LTP induction experiments in the presence of picrotoxin ($GABA_A$ antagonist) to maximize tetanus-induced depolarization and NMDAR activation. Similar to the experiments in the absence of picrotoxin, there was a significant difference between groups, with field potentials returning to baseline at later time points in slices from GluN2B KO mice [$t(9) = 2.790$; $P < 0.05$; Fig. 3*B*]. Another potential explanation for the lack of LTP in GluN2B KO mice is occlusion attributable to enhanced release probability in these KO mice. Therefore, to add support for the idea that the GluN2B subunit was required for LTP, we assessed the impact of pharmacological inhibition of GluN2B-containing NMDARs on BNST LTP in naive C57BL/6J mice. GluN2B antagonism by application of 10 μM Ro25-6981 before tetanization prevented significant LTP induction (Fig. 3*C*). There was no significant difference in the field potential during the first 10 min following tetanus between drug- and non–drug-treated controls [$t(11) = 0.758$; P = N.S.]. However, at later time points (51–60 min following tetanus), there was a significant difference between slices treated with GluN2B antagonist and nondrug controls [$t(11) = 4.061$; $P < 0.005$]. Application of the GluN2B antagonist caused field potentials to return to baseline, whereas nondrug controls remained potentiated. This 10-μM dose of Ro25-6981 alone (1-h application) caused no significant change from baseline on field potentials [$t(4) = 0.4346$; P = N.S.]. These results demonstrate that the GluN2B subunit is necessary for LTP in dlBNST.

Lack of Acute Ethanol Sensitivity on NMDAR EPSCs in GluN2B KO Mice. Ethanol (100 mM) has previously been shown to decrease evoked NMDAR EPSC peak amplitude in the ventral BNST (vBNST) (24), as well as inhibiting NMDAR-isolated field potentials in dlBNST (25). Consistent with these findings, we observed in control mice that 100 mM ethanol produced a decrease of ∼50% in NMDAR EPSC peak amplitude in dlBNST [$t(7) = 6.823$; $P < 0.0005$; Fig. 4 *A* and *C*]. This effect of ethanol was absent in slices prepared from GluN2B KO mice [$t(7) = 0.367$; P = N.S.; Fig. 4 *A–C*]. Importantly DL-2-Amino-5-phosphonopentanoic acid (DL-APV) (100 μM), an NMDAR antagonist, was still able to cause a sizable inhibition of the NMDAR EPSC peak amplitude in GluN2B KO mice [$t(2) = 22.74$; $P < 0.005$; Fig. 4 *B* and *C*], illustrating that NMDAR current is still present yet ethanol-insensitive. Similarly, we demonstrated that in the presence of GluN2B pharmacological antagonism using 10 μM Ro25-6981, there was no effect of 100 mM ethanol on NMDAR EPSC peak amplitude [$t(4) = 0.2607$; P = N.S.; Fig. 4*D*]. Further, we found that ethanol sensitivity of NMDAR-isolated field potentials in dlBNST is retained in slices prepared from GluN2A KO mice [$t(12) = 0.413$; P = N.S.; Fig. 4*E*]. These data demonstrate that the GluN2B subunit plays a critical role in mediating acute inhibitory effects of ethanol on dlBNST NMDARs.

Chronic Intermittent Ethanol Exposure Produces GluN2B-Dependent Enhancement of LTP. Initial studies were performed to determine the effects of chronic intermittent ethanol (CIE; two 4-d cycles of intermittent ethanol vapor; diagram in Fig. 5*A*) on LTP in dlBNST in naive C57BL/6J mice. In these experiments, there was no difference at early time points [$t(15) = 0.085$; P = N.S.] but a significant enhancement in the amount of potentiation at the late time point [$t(15) = 3.909$; $P < 0.005$; Fig. 5*B*] in ethanol-exposed mice compared with their air-exposed counterparts.

To investigate the role of GluN2B in these chronic effects of ethanol, control and GluN2B KO mice were also exposed to CIE, and LTP in dlBNST was evaluated during withdrawal. During withdrawal, there was a significant difference in both the early [$t(12) = 5.587$; $P < 0.001$] and late [$t(12) = 3.356$; $P < 0.01$; Fig. 5*C*] time points following the LTP induction protocol between control and GluN2B KO mice. Notably, there was no change in the amount of LTP in slices from GluN2B KO mice with or without chronic ethanol exposure, demonstrating that the enhanced potentiation seen in controls and C57BL/6J mice is GluN2B-dependent.

Pharmacological Modulation of Extrasynaptic GluN2B-Containing NMDARs. The enhancement of GluN2B-dependent glutamate transmission following chronic ethanol could be a result of signaling through synaptic and/or extrasynaptic GluN2B-containing NMDARs in dlBNST. To dissociate the contributions of these different receptor populations, we took advantage of divergent actions of Ro25-6981 on NMDAR function. Although ifenprodil derivatives, such as Ro25-6981, are well known for their ability to inhibit GluN2B-containing synaptic NMDARs noncompetitively, it has also been shown that a consequence of the binding of ifenprodil and its derivatives is an enhancement of glutamate affinity for the NMDAR (43, 44). Thus, under low-glutamate concentrations (as would be found at extrasynaptic receptors), this leads to an enhanced agonist-induced NMDAR current (43, 45, 46). We

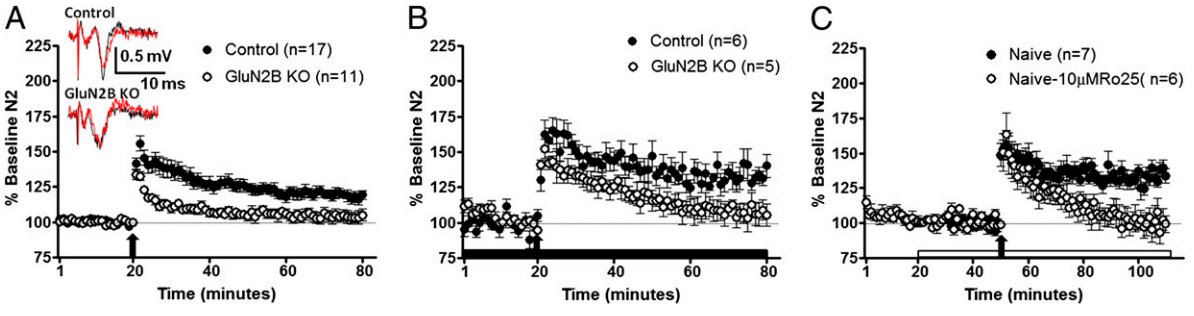

Fig. 3. GluN2B is necessary for LTP in dlBNST. (*A*) Averaged time course of synaptic field potentials after high-frequency stimulation (at arrow; two 1-s trains at 100 Hz) in dlBNST from GluN2B KO and control (single-transgene and WT littermates) mice. (*Inset*) Representative traces of control and GluN2B KO mice before tetanus (red) and 60 min after tetanus (black). (*B*) Averaged time course of synaptic field potentials after high-frequency stimulation (at arrow; two 1-s trains at 100 Hz) in dlBNST from GluN2B KO and control (single-transgene and WT littermates) mice in the presence of picrotoxin (25 μM). (*C*) Averaged time course of synaptic field potentials after high-frequency stimulation (at arrow; two 1-s trains at 100 Hz) in dlBNST from naive adult male C57BL/6J mice. RO25-6981 (10 μM, a GluN2B-selective antagonist) was applied 30 min before tetanus and throughout the remainder of the experiment.

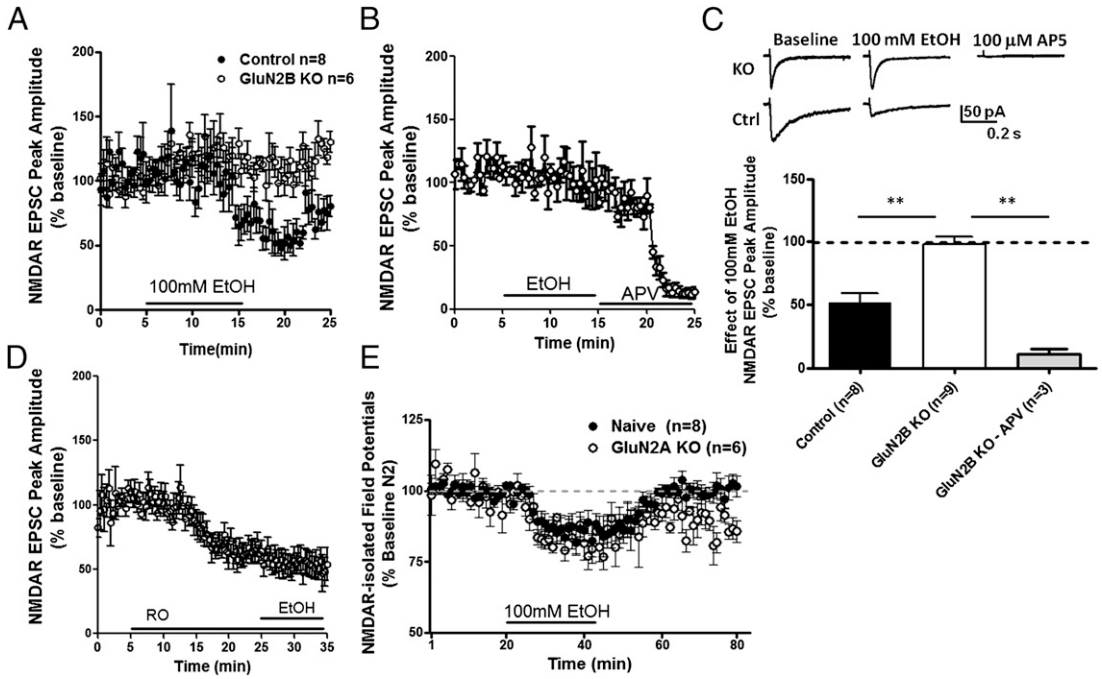

Fig. 4. Lack of acute ethanol sensitivity on NMDAR EPSCs in GluN2B KO mice. (*A*) Time course of peak amplitudes from evoked NMDAR EPSCs during 10-min treatment of ethanol (100 mM) in dlBNST neurons of GluN2B KO and control (single-transgene and WT littermates) mice. (*B*) Time course of evoked NMDAR EPSCs during 10-min treatment of ethanol (100 mM), followed by 10-min application of DL-APV (100 μM) in dlBNST neurons of GluN2B KO mice. (*C*) Summary of NMDAR EPSC peak amplitude during ethanol application (10 min) in GLuN2B KO and control mice and during DL-APV in GLuN2B KO mice. $^{**}P < 0.01$. (*D*) Time course of peak amplitudes from evoked NMDAR EPSCs during 20-min pretreatment of Ro25-6981, followed by 10-min application of ethanol (100 mM) in dlBNST neurons of naive mice. (*E*) Averaged time courses of NMDAR-isolated synaptic field potentials in dlBNST during 15-min treatment of ethanol (100 mM) from naive C57BL/6J and GluN2A KO mice.

took advantage of our ability to record synaptically evoked NMDAR-mediated field potentials in dlBNST to explore this phenomenon. Because these field potentials are evoked under zero $Mg2^{+}$ conditions and use larger stimulus intensities to evoke measureable responses, it is likely that both synaptic and extrasynaptic NMDARs are recruited, as was previously demonstrated with similar techniques in the striatum (47). As would be expected for an NMDAR-dependent response, evoked NMDAR field potentials are blocked by the competitive NMDAR antagonist DL-APV [$t(8) = 11.97$; $P < 0.0001$; Fig. 6*A*], as previously reported (25). However, the effects of Ro25-6981 were bimodal and dose-dependent. Ro25-6981 at a dose of 10 μM caused ~50% inhibition of NMDAR field potentials [$t(6) = 10.92$; $P < 0.0001$; Fig. 6*B*] consistent with its GluN2B-selective antagonizing properties and its actions on LTP in dlBNST (Fig. 3*C*). In contrast, Ro25-6981 at a dose of 2 μM (but not 0.2 μM) produced an enhancement of NMDAR transmission, likely attributable to the enhancement of glutamate affinity at extrasynaptic sites [$t(7) = 5.741$; $P < 0.001$; Fig. 6*B*]. This effect was mimicked by ifenprodil [10 μM; $t(4) = 3.48$; $P < 0.05$] but not prazosin [10 μM; $t(3) = 0.21$; P = N.S.], which antagonizes α1-adrenergic receptors that are also bound by ifenprodil derivatives (37). The enhancement of NMDAR trans-

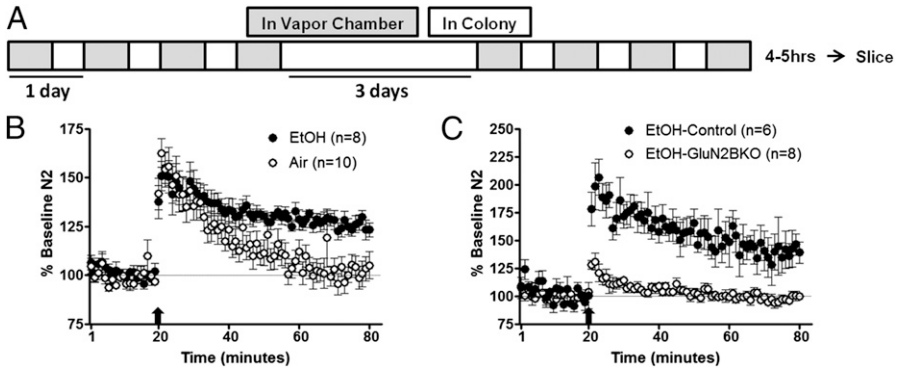

Fig. 5. Chronic ethanol treatment enhances excitatory transmission, and this effect is GluN2B-dependent. (*A*) Two cycles of CIE exposure; each cycle consists of 4 d of 16 h in ethanol or air vapor chambers (gray boxes) and 8 h out of vapor chambers (white boxes; withdrawal). Recordings were performed 4–5 h after the final chamber exposure. (*B*) Averaged time course of synaptic field potentials after high-frequency stimulation (at arrow; two 1-s trains at 100 Hz) in dlBNST from naive adult male C57BL/6J mice after chronic ethanol or air treatment. (*C*) Averaged time course of synaptic field potentials after high-frequency stimulation (at arrow; two 1-s trains at 100 Hz) in dlBNST from GluN2B KO and control (single-transgene and WT littermates) mice after chronic ethanol or air treatment.

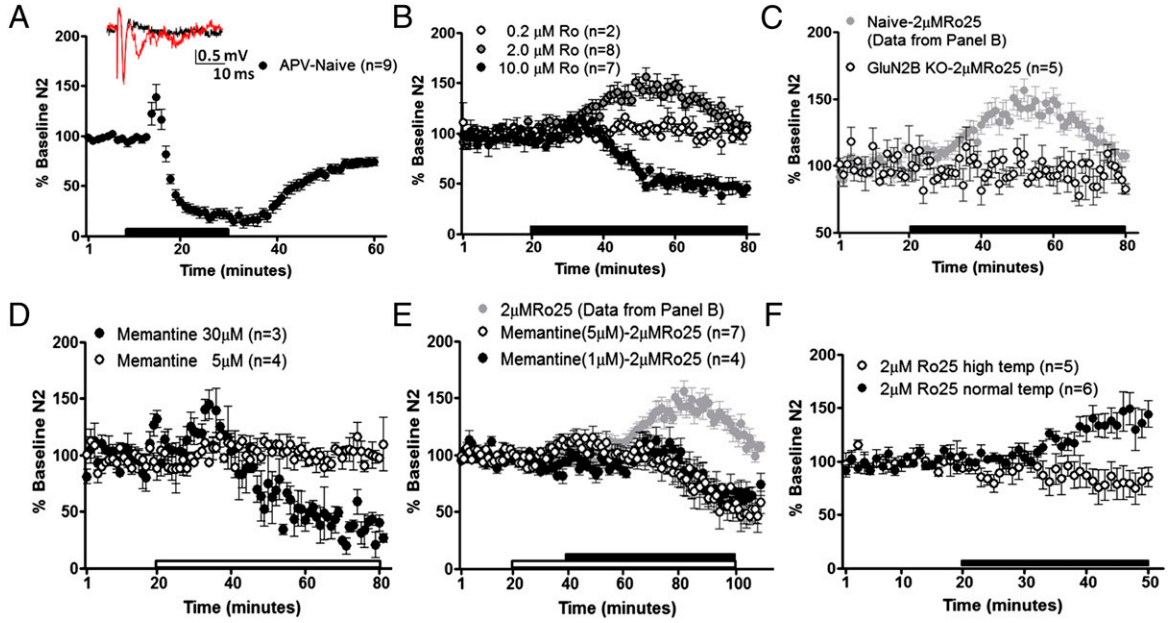

Fig. 6. RO25-6981 (2.0 μM) enhances evoked NMDAR responses through extrasynaptic GluN2B-containing NMDARs. Averaged time courses of NMDAR-isolated synaptic field potentials in dlBNST following 20 min of DL-APV (100 μM) in slices from naive adult male C57BL/6J mice (*A*), 60 min of Ro25-6981 (0.2, 2.0, or 10 μM) in slices from naive adult male C57BL/6J mice (*B*), 60 min of 2.0 μM Ro25-6981 in slices from GluN2B KO mice and representative data of 2.0 μM Ro25-6981 from *B* (*C*), 60 min of memantine (5 or 30 μM) in naive adult male C57BL/6J mice (*D*), memantine (1 or 5 μM) 20 min before and during 60 min of 2.0 μM Ro25-6981 in slices from naive adult male C57BL/6J mice (E), and representative data of 2.0 μM Ro25-6981 alone from *B* and 30 min of 2.0 μM Ro25-6981 in slices from naive adult male C57BL/6J mice under normal temperature (temp; ~29 °C) or high temperature (~36 °C) (*F*).

mission by 2 μM Ro25-6981 was specific for GluN2B-containing NMDARs, because the effect was absent in slices from GluN2B KO mice [$t(4) = 0.4768$; P = N.S.; Fig. 6*C*].

To provide additional support for the idea that 2 μM Ro25-6981 enhances NMDAR transmission by increasing glutamate affinity at extrasynaptic NMDARs, we evaluated its actions in the presence of memantine. A number of studies have provided evidence that the low-affinity NMDAR antagonist memantine preferentially antagonizes extrasynaptic NMDARs at low doses (48–51). In isolated NMDAR fields in dlBNST, 30 μM memantine reduced evoked NMDA field potentials [$t(2) = 8.325$; $P < 0.05$; Fig. 6*D*]. A lower concentration (5 μM) of memantine did not have a detectable effect on the evoked NMDAR field potential [$t(3) = 0.3609$; P = N.S.; Fig. 6*D*]; however, when this low dose of memantine was applied before and during application of 2 μM Ro25-6981, memantine blocked the enhancement of NMDAR transmission [1 μM: $t(3) = 1.515$, P = N.S.; 5 μM: $t(6) = 1.367$, P = N.S.; Fig. 6*E*], returning the antagonistic effects of Ro25-6981 [1 μM: $t(3) = 3.458$, $P < 0.05$.; 5 μM: $t(6) = 5.05$, $P < 0.005$; Fig. 6*E*].

As another test that Ro25-6981–induced facilitation of NMDAR field potentials reflects recruitment of extrasynaptic NMDARs, we examined the temperature dependence of this phenomenon. Glutamate transport is highly temperature-dependent, such that at higher temperatures, glutamate clearance becomes much more efficient (52, 53). Thus, under these conditions, it would be predicted that extrasynaptic receptors would not be occupied by glutamate and that Ro25-6981 would not facilitate NMDAR responses. As predicted, raising the temperature to ~36 °C removed the ability of Ro25-6981 to enhance evoked NMDAR responses [29 °C: $t(5) = 2.858$, $P < 0.05$; 36 °C: $t(4) = 1.585$, P = N.S.; Fig. 6*F*]. In total, these results suggest that the enhancing effects of 2 μM Ro25-6981 are through actions at extrasynaptic NMDARs.

Enhancement of GluN2B-Containing Extrasynaptic NMDARs Following Chronic Ethanol. Recent data have provided evidence that withdrawal from chronic ethanol exposure produces a significant increase in GluN2B-containing extrasynaptic NMDARs (35). To determine whether these receptors play a role in modulating synaptic plasticity in the BNST, we assessed the effects of 2 μM Ro25-6981 on LTP in slices taken from air- and CIE-withdrawn C57BL/6J mice. Interestingly, we found that Ro25-6981 (2 μM) significantly enhanced LTP elicited in slices taken from CIE-withdrawn mice, although it had no effect on LTP in slices taken from air-treated mice [$F(5,39) = 7.32$; $P < 0.0001$; Fig. 7 *A*, *B*, and *D*] or naive C57BL/6J mice [$t(12) = 2.10$; P = N.S.]. This 2-μM dose of Ro25-6981 alone caused no significant change in field potentials from nondrug baseline in slices from ethanol-treated [$t(7) = 1.742$; P = N.S.] or naive [$t(5) = 0.6256$; P = N.S.] mice. To provide additional support that this enhancement was caused by actions at extrasynaptic NMDARs, 5 μM memantine was applied either alone or before and in conjunction with low-dose Ro25-6981 following chronic ethanol exposure. This memantine pretreatment significantly blocked the Ro25-6981–induced enhancement of LTP (Fig. 7 *C* and *D*), whereas memantine alone produced a nonsignificant trend for reduced LTP in ethanol-treated mice. Finally, to ascertain if this enhanced LTP by Ro25-6981 in ethanol-treated mice was a result of increased transmission at extrasynaptic GluN2B, we evaluated the effects of 2 μM Ro25-6981 on isolated NMDAR field potential in slices from naive, air-treated, and ethanol-treated mice. In these experiments, there was no significant difference in the peak effect of Ro25-6981 between the treatment conditions [$F(2,18) = 0.2756$; P = N.S.]. These results suggest (*i*) that the enhancement of LTP in ethanol-treated mice is a result of signaling mechanisms downstream of extrasynaptic NMDARs and/or (*ii*) that there could have been a ceiling effect for the measurement of extrasynaptic NMDAR function in these experiments (2 μM Ro25-6981 on isolated NMDAR field potentials), such that no further enhancement from Ro25-6981 could be seen in ethanol-treated mice. Collectively, these data indicate that CIE enhances extrasynaptic GluN2B-containing receptors

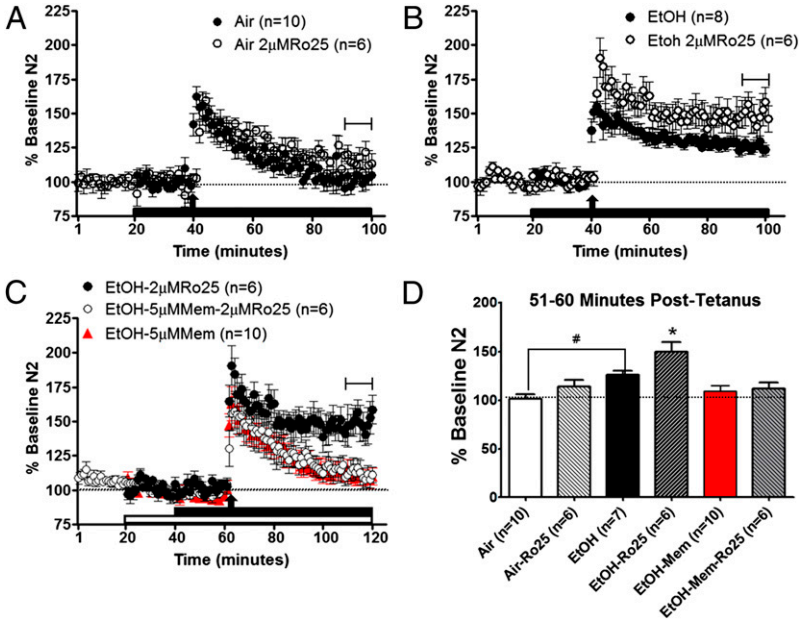

Fig. 7. RO25-6981 (2.0 μM) enhances LTP only after chronic ethanol treatment. Averaged time course of synaptic field potentials after high-frequency stimulation (at arrow; two 1-s trains at 100 Hz) in dlBNST from either air-treated (*A*) or ethanol-treated (*B* and *C*) adult male C57BL/6J mice. Ethanol- and air-treated mice were given two cycles of CIE exposure, in which each cycle consists of 4 d of 16 h in ethanol or air vapor chambers and 8 h out of vapor chambers (withdrawal). Recordings were performed 4–5 h after the final chamber exposure in these groups. Low-dose Ro25-6981 (2 μM, a GluN2B-selective antagonist) was applied 20 min before tetanus and throughout the remainder of the experiment. (*C*) Memantine (5 μM, an NMDA antagonist) was applied 20 min prior either alone or during low-dose Ro25-6981. Tetanus was applied 20 min after Ro25-6981 application. (*D*) Summary graph of averaged field potentials 51–60 min after tetanus (from time courses in *A*–*C*). $^{*}P < 0.05$ from all groups; $^{\#}P < 0.05$ between air and EtOH.

and that this receptor population functions to facilitate LTP in dlBNST.

Discussion

These studies indicate a key role for GluN2B in dlBNST, both in basal regulation of glutamate synapses and plasticity as well as in acute and chronic ethanol regulation of these synapses. Further, these data suggest the intriguing possibility that at least a portion of the glutamatergic enhancement produced by chronic ethanol in dlBNST may be attributable to unique actions of extrasynaptic GluN2B-containing receptors positively regulating LTP. Thus, these data suggest that GluN2B in dlBNST likely plays important roles in alcohol-related behaviors. Using the identical transgenic strategy, Badanich et al. (41) found that GluN2B deletion dramatically increased behavioral sensitivity to acute alcohol, suggesting these receptors play an important role in modulating ethanol-related behaviors.

Disrupted Glutamate Transmission in Conditional GluN2B KO Mice. The current breeding strategy resulted in an almost complete (~80%) reduction in GluN2B expression in dlBNST. This resulted in a selective alteration of glutamate receptors at synapses in dlBNST, since GluN2A subunits and the AMPAR subunit GluA1 were unchanged. GluN2B KO mice had reduced GluN1 and CaMKIIβ levels in dlBNST, which is logical considering that GluN1 requires other NMDAR subunits for heteromeric assembly and CaMKII is an intracellular protein commonly associated with GluN2B-containing receptors (54–56). This pattern of subunit adaptations was similar to previously reported work with GluN2B knockdown mice (7, 41, 42). Consistent with this deletion of GluN2B, the decay kinetics of evoked NMDAR-EPSCs were significantly shortened and AMPA/NMDA ratios in KO mice were substantially enhanced. Because these ratios were isolated based on decay times of AMPAR- and NMDAR-mediated responses rather than pharmacological isolation, they could be affected by kinetic changes. Synaptic AMPARs appear grossly normal, because sEPSC amplitude and levels of GluA1 were not altered. However, an increase in sEPSC frequency and a decrease in evoked EPSC PPR suggests that basal glutamate release probability is increased in KO mice. There are a number of potential causes for this enhanced glutamate release, which may reflect a compensation for the loss of postsynaptic GluN2B signaling.

GluN2B-Dependent LTP. We previously reported that GluN2A was dispensable for LTP in dlBNST (39). Using GluN2B KO mice as well as the GluN2B antagonist Ro25-6981, we find that LTP in dlBNST requires this NMDAR subunit. These data are consistent with a large body of evidence suggesting an obligatory role for GluN2B in LTP in other brain regions (57–60). However, they are inconsistent with other studies using pharmacological approaches (61–65) and other GluN2B KO lines (7, 42), where only partial reductions of LTP were observed. As has been noted in several reviews, the use of GluN2B- and GluN2A-selective ligands is fraught with complications because of many complex mechanisms (36, 38). In regard to the comparison of the present dataset with other data from GluN2B KO mice in the hippocampus, several things may account for these differences. First, the reduction of GluN2B achieved in the studies by Brigman et al. (7) and von Engelhardt et al. (42) was more modest than that achieved within dlBNST in the present breeding strategy. Second, previous studies in the juxtacapsular nucleus of the BNST have emphasized that LTP observed using field potential recordings of this portion of the BNST represents cellular, rather than synaptic, plasticity, which may require fundamentally distinct mechanisms (26). Although this cannot be ruled out as a possibility, at present, our recordings are medial to the juxtacapsular nucleus, which is an extremely narrow nucleus (~75 μM in width) adjacent to the striatum. Nonetheless, regionally specific differences in plasticity mechanisms have been noted repeatedly in the literature. Aside from these regional differences, it could also be argued that lack of LTP

in GluN2B KO mice might be a result of reduced NMDAR transmission and not selective to GluN2B loss. This interpretation is plausible. However, previous work in dlBNST found that 10-min APV application was ineffective in reducing LTP even though it produces ~75% inhibition of NMDAR transmission (Fig. 6*A*). Further, when APV was applied in GluN2B KO mice during acute ethanol experiments (Fig. 4 *B* and *C*), there was still substantial NMDAR inhibition, demonstrating that considerable NMDAR transmission remains in GluN2B KO mice. Another possibility is that because GluN2B KO mice have enhanced glutamate release, LTP is occluded in slices from these mice. Although the occlusion of LTP is a valid possibility, unaltered sEPSC amplitude in GluN2B KO mice and a similar lack of LTP with pharmacological blockade of the GluN2B subunit make this option less likely. In sum, our data demonstrate that LTP in dlBNST heavily depends on GluN2B.

GluN2B-Dependent Effects of Acute and Chronic Ethanol. The second unique finding in this work is that acute ethanol inhibition in dlBNST requires the GluN2B subunit. Here, we demonstrate that 100 mM ethanol, a concentration that produces a large inhibition of NMDAR EPSCs in this region, has no detectable effect in GluN2B KO mice. These data lend strong support to a growing body of literature indicating a key role for GluN2B in many ethanol-dependent processes (18, 19, 21, 63). They also are consistent with recent data suggesting that unique Tyr phosphorylation sites on GluN2B play key roles in the ethanol sensitivity of NMDARs in vivo (66). However, they are inconsistent with strong recombinant data in cell lines indicating that most combinations of NMDARs exhibit ethanol sensitivity in vitro (67–70). We cannot rule out the possibility that presently unknown compensations in the KO mice produced adaptations at glutamate synapses that rendered NMDAR currents ethanol-insensitive. However, in current and previous studies, we have shown that preapplication of the GluN2B-selective antagonist Ro25-6981 also removes ethanol sensitivity in a wild-type mouse (24). We also should point out that in brain slice studies, ethanol is typically bath-applied to assess its actions on NMDAR function, whereas typical in vitro studies use more rapid means of alcohol delivery and assess currents induced by agonist application. Thus, it is possible that these two approaches target distinct forms of ethanol sensitivity. Further, the divergence in these findings could be attributable to differences between dendritic and somatic populations, because isolated cell preparations mainly measure somatic populations. Finally, it is also possible that the key molecules necessary for determining NMDAR ethanol sensitivity in the brain are not present in isolated systems. In sum, our present data indicate that GluN2B plays a critical role in determining acute ethanol sensitivity of NMDARs in dlBNST.

In the present work, we also found that CIE produced an enhancement of LTP in dlBNST compared with sham-treated mice, and that this also was ablated in GluN2B KO mice. This finding of enhanced LTP was not altogether surprising, given the known hyperexcitability of glutamate synapses and NMDARs during withdrawal from chronic ethanol (71, 72). This enhanced NMDAR activity is thought to arise mainly from increased expression of NMDAR subunits after chronic ethanol administration (28–33). Several studies also suggest that this increased NMDAR function from chronic ethanol could lead to enhancements in plasticity. For example, in the vBNST, an increase in temporal summation of NMDAR EPSCs was produced from a modest chronic ethanol exposure of 4 d (27). Increases in NMDAR EPSC temporal summation have been shown in the visual cortex to decrease the threshold required to produce NMDAR-dependent plasticity (73). It is also important to note that alcohol effects on LTP of field potential responses have been explored in the neighboring juxtacapsular nucleus, where chronic alcohol exposure more predominantly led to a decrease in LTP with protracted withdrawal (26). Comparing our data with these studies could indicate subregional differences in the actions of ethanol, although substantial differences in ethanol delivery and in species used may also account for the differences.

It is important to note that although there was a significant enhancement in ethanol-treated mice compared with air-treated controls, there was also a somewhat blunted LTP in air-treated mice (compared with LTP in naive C57BL/6J mice; Fig. 3*C*). This effect is likely a consequence of mild stress from vapor procedures (repeated injections, pyrazole administration, and exposure to novel inhalation chambers). Previous studies have shown that LTP in dlBNST can be blunted by different stressors (74). This effect in air-treated mice implies that enhancement in LTP after chronic ethanol might be larger if the blunting factor of stress were removed. A further consequence of this is that the amount of LTP in ethanol-treated and naive mice is not significantly different. Thus, it could be argued that ethanol is merely blocking these stress effects and has no pharmacological effects on LTP in this region. This idea, however, is negated by the data showing that low-dose Ro25-6981 potentiates LTP following chronic ethanol but has no effect in slices from naive mice. Given that these data illustrate an ethanol-specific change compared with naive mice, we argue that the enhancement of LTP in ethanol-treated groups compared with air is the consequence of a pharmacological effect of ethanol. Thus, we postulate that stress reduces the amount of LTP in both treatment conditions equally. Additionally, although ethanol clearly has anxiolytic properties, this CIE exposure and withdrawal have been mainly associated with adaptations in behavioral anxiogenesis rather than anxiolysis.

The enhancement of LTP that we observed following CIE required GluN2B, demonstrated by a lack of potentiation in dlBNST following CIE in slices prepared from GluN2B KO mice. As with the acute effects of ethanol, there is also a substantial amount of literature suggesting the GluN2B is involved in the chronic effects of ethanol. In the extended amygdala, blockade with GluN2B antagonist produced more robust effects after chronic ethanol (27, 75). As mentioned previously, there are a large number of studies that find increases in mRNA and/or protein of GluN2B after chronic ethanol (27–33). It is important to note that NMDAR (specifically GluN2B) expression is upregulated during chronic ethanol and acute withdrawal. In contrast, during protracted withdrawal (1 wk), GluN1 and GluN2B levels were actually decreased (76). Future studies investigating these NMDAR subunits during more protracted periods of withdrawal will be critical in evaluating potential therapeutic agents for treating alcohol relapse.

Role of Extrasynaptic GluN2B-Containing Receptors in Plasticity and Chronic Ethanol Effects. NMDARs are known to exist in both synaptic and extrasynaptic populations. Evidence suggests that these two populations of NMDARs differentially regulate neuronal physiology and plasticity. Extrasynaptic NMDAR populations are thought to be heavily populated by GluN2B-containing NMDARs. Thus, our data would suggest that these receptors are important targets of ethanol. Chronic ethanol exposure has been reported to enhance the clustering of synaptic NMDARs into dendritic spines (34). However, recent work has also suggested that there is lateral movement of GluN2B-containing receptors from synaptic to extrasynaptic populations in hippocampal neurons during withdrawal (35). These data demonstrate there is a time dependence (during ethanol exposure vs. withdrawal) to the localization of GluN2B that likely has important functional consequences.

In the present study, we have used the unique actions of Ro25-6981 on NMDARs to explore the contributions of extrasynaptic NMDARs to plasticity in CIE-treated mice. A consequence of Ro25-6981 interaction with GluN2B-containing NMDARs is that affinity for glutamate is increased (43), such that under conditions of low agonist availability, NMDAR currents are enhanced.

Extrasynaptic NMDARs would be predicted to see much lower concentrations of glutamate than synaptic NMDARs. Previous studies have demonstrated that the use of optimized conditions (low Mg and high stimulus intensities) to explore evoked NMDAR responses can lead to recruitment of these receptors (47). Several lines of evidence indicate that the enhanced NMDAR response we observe with 2 μM Ro25-6981 under our recording conditions is mediated by extrasynaptic receptors: (*i*) It is mimicked by ifenprodil and is not present in slices from GluN2B KO mice; (*ii*) it is blocked by the extrasynaptic NMDAR-preferring memantine at concentrations that do not alter the basal response; and (*iii*) it is not observed at higher temperatures, where glutamate transport is more efficient.

Our findings using 2 μM Ro25-6981 suggest that extrasynaptic GluN2B-containing receptors uniquely facilitate LTP after ethanol withdrawal, because a submaximal concentration of Ro25-6981 paradoxically enhances LTP in CIE-treated but not air-treated or naive mice. This could be attributable to a couple of possibilities, including altered expression level of extrasynaptic receptors or changes in the signaling molecules that this population of receptors interacts with. This is distinct from work primarily in the cortex and hippocampus, which has largely found that extrasynaptic GluN2B receptors contribute more to promote long-term depression (LTD) vs. LTP (64, 65). Despite these regional differences in plasticity modulation, a large body of work confirms that extrasynaptic GluN2B is involved in excitotoxic processes and implicated in a number of pathological conditions [e.g., Huntington disease, ischemia, Parkinson disease, Alzheimer's disease (77, 78)]. The examination of these data in this larger context leads us to speculate that the term "extrasynaptic" likely does not define a single population of NMDARs but, instead, a group of functionally and anatomically distinct receptors. It is important to note that although the Ro25-6981 data suggest that extrasynaptic NMDARs positively modulate LTP in CIE-withdrawn mice, it is unclear whether they also participate in the enhancement of LTP we observe between CIE and sham mice. For example, as Carpenter-Hyland et al. (34) demonstrated in hippocampal neurons, it is possible that increased synaptic incorporation of NMDARs is responsible for increased LTP. Regardless, these data demonstrate a GluN2B-dependent facilitation of LTP in dlBNST by CIE.

This work has demonstrated a clear role of GluN2B in plasticity and alcohol-related effects in the BNST, a region critical in modulating behaviors involved in relapse. Although subunit specificity of ethanol effects are critical, these data also make it clear that the localization of these receptors is key in their functionality; thus, the development of therapeutic agents with subunit and/or localization specificity are likely to be effective in preventing relapse in patients with alcohol use disorders. One such drug, memantine, seems to display some localization specificity and is currently under active investigation as a treatment for alcoholism. Interestingly, it has been shown to reduce reports of withdrawal severity (79). Our data suggest that effectiveness of this compound may be greatest in alcohol use disorders in withdrawn-dependent alcoholics, in whom an extrasynaptic, more memantine-sensitive population of receptors exists.

Materials and Methods

Animals. Male C57BL/6J (6–8 wk of age; Jackson Laboratories), GluN2B KO, GluN2A KO, or genetic control (described below) mice were housed in groups of two to five. Food and water were available ad libitum. All procedures were approved by the Animal Care and Use Committee at Vanderbilt University. GluN2A KO mice were provided by Integrative Neuroscience Initiative on Alcoholism (INIA) Stress Consortium (Vanderbilt University, Nashville, TN).

Generation of GluN2B KO Mice. Homozygous GluN2B-floxed mice were generated as previously described (7) and crossed with promoter from human cytomegalovirus (phCMV)-tetO-CRE or CaMKIIα-tTA transgene hemizygous mice as previously described (41). These mice were mated with mice hemizygous for the complementary transgene to produce KO mice and controls as previously described (41) (Fig. 1*A*). The CaMKIIα promoter fragment limits expression of tTA largely to postnatal forebrain, avoiding lethality associated with the constitutive GluN2B KO mice previously produced (40).

Western Blots. Punches were sonicated in 2% (wt/vol) SDS, 10 mg/mL aprotinin, and 10 mg/mL leupeptin. Whole homogenate was analyzed. Protein levels were determined with a BCA protein assay kit, diluted to equal concentrations, mixed with sample buffer [62.5 mM Tris·Cl (pH 6.8), glycerol, 5% (wt/vol) SDS, 0.5% bromophenol blue, and 5% (vol/vol) β-mercaptoethanol], and 20 μg was run on a 10% (vol/vol) polyacrylamide-resolving gel. Protein was transferred either to a single nitrocellulose membrane or to two Immobilon PVDF membranes (Pall Corporation) in series. The nitrocellulose membrane was stained for total protein with Ponceau S. For the PVDF blots, the first membrane was probed with specific primary antibodies, whereas the second membrane was stained for total protein using colloidal gold (Bio-Rad) to verify equal lane loading grossly. Membranes were either cut at the appropriate molecular weight and probed for different antibodies or stripped and reprobed with additional primary antibodies. Antibodies used include mouse GluN2B (no. 610417; BD Biosciences), mouse GluN1 (no. 556308; BD Biosciences), rabbit GluN2A (no. 07-632; Millipore), mouse CaMKIIα (no. MA1-048; Thermo/Fisher), CaMKIIβ (no. 139800; Invitrogen), pan-goat CaMKII (80), and GluA1 (no. SC-55509; Santa Cruz). To combine blocks of experiments from different blots, samples on each blot were normalized to their experimental time point control.

Slice Preparation. Mice were transported from the animal colony to the laboratory and placed in sound-attenuated cubicles for 1 h before slicing. They were then decapitated under isoflurane. The brains were quickly removed and placed in ice-cold sucrose artificial cerebrospinal fluid (ACSF): 194 mM sucrose, 20 mM NaCl, 4.4 mM KCl, 2 mM $CaCl_2$, 1 mM $MgCl_2$, 1.2 mM NaH_2PO_4, 10.0 mM glucose, and 26.0 mM $NaHCO_3$ saturated with 95% O_2/5% CO_2 (vol/vol). Slices 300 μm in thickness were prepared using a Tissue Slicer (Leica). Slices containing anterior portions of dlBNST (bregma, 0.26–0.02 mm) were selected using the internal capsule, anterior commissure, and stria terminalis as landmarks.

Whole-Cell Recordings. After dissection, slices were transferred to a holding chamber containing heated (~29 °C), oxygenated (95% O_2/5% CO_2, vol/vol) ACSF [124 mM NaCl, 4.4 mM KCl, 2 mM $CaCl_2$, 1.2 mM $MgSO_4$, 1 mM NaH_2PO_4, 10.0 mM glucose, and 26.0 mM $NaHCO_3$ (pH 7.2–7.4); 290–310 mOsm]. Recording electrodes (3–6 MΩ) were pulled on a Flaming/Brown Micropipette Puller (Sutter Instruments) using thin-walled borosilicate glass capillaries. EPSCs were evoked by local fiber stimulation with bipolar Ni-chrome electrodes. Stimulating electrodes were placed in the stria terminalis and 100–300 μm dorsal to the recorded neuron. Electrical stimulation (5–25 V with a duration of 100–150 μs) was applied at 0.1 Hz. Recording electrodes were filled with 117 mM Cs + gluconate, 20 mM Hepes, 0.4 mM EGTA, 5 mM tetraethylammonium, 2 mM $MgCl_2$, 4 mM ATP, and 0.3 mM GTP (pH 7); 285–290 mOsm. AMPAR EPSCs and sEPSCs were isolated by adding 25 μM picrotoxin and recording at a holding potential of −70 mV in normal ACSF. For AMPA/NMDA ratio measurements, the peak amplitude of AMPAR-mediated responses measured at −70 mV was divided by the amplitude of the dual component at +40 mV, 40–50 ms after onset of the current. This is a time point when the AMPAR component is negligible. In PPR experiments, paired evoked 100- to 200-pA responses at 0.05 Hz were elicited and the stimulus interval was varied from 20 to 140 ms by 20-ms steps. Signals were acquired via a Multiclamp 700B amplifier (Axon Instruments), and were digitized and analyzed via pClamp 10.2 software (Axon Instruments). Input resistance, holding current, and series resistance were all monitored continuously throughout the duration of experiments. Experiments in which changes in series resistance were greater than 20% were not included in the data analysis. Experiments were analyzed by measuring peak amplitude of the synaptic response, which was then normalized to the baseline period. NMDAR EPSCs were isolated in Mg-free ACSF [124 mM NaCl, 4.4 mM KCl, 3.7 mM $CaCl_2$, 1 mM NaH_2PO_4, 10 mM glucose, and 26 mM $NaHCO_3$ (pH 7.2–7.4); 290–310 mOsm] with picrotoxin (25 μM) and 2,3-dihydroxy-6-nitro-7-sulfamoyl-benzo[f]quinoxaline-2,3-dione (NBQX) (10 μM) and recorded at a holding potential of −70 mV.

Field Potential Recordings. After dissection, slices were transferred to an interface recording chamber, where they were perfused with heated (~29 °C) and oxygenated (95% O_2/5% CO_2, vol/vol) ACSF at a rate of about 2 mL/min. Slices were allowed to equilibrate in ACSF for at least 1 h before experiments began. A bipolar stainless-steel stimulating electrode and a borosilicate glass recording electrode filled with ACSF were placed in dlBNST to elicit and record an extracellular field response. Baseline responses to a stimulus (50 μs) at an

intensity that produced ~40% of the maximum response were recorded for 20 min at a rate of 0.05 Hz. After acquisition of a stable baseline, LTP was induced with two trains of 100-Hz, 1-s tetanus delivered with a 20-s intertrain interval at the same intensity as baseline test pulses. The N1 (an index of sodium channel-dependent firing) was also monitored, and experiments in which it changed by more than ~20% were discarded. Analyses were made from the percent change of the N2 from baseline 0–10 min after tetanus and 51–60 min after tetanus. In LTP experiments with Ro25-6981 (2 or 10 μM), the compound was applied after 20 min of stable baseline and remained throughout the duration of the experiment. The tetanus was delivered after 20 min (2-μM experiments) or 30 min (10-μM experiments) of Ro25-6981 baseline. In memantine and Ro25-6981 experiments, memantine was applied after 20 min of stable baseline and Ro25-6981 (2 μM) was then coapplied for an additional 20 min of drug baseline. Tetanus was then delivered, and both drugs remained in the bath solution throughout the remainder of the experiment.

In other field experiments, NMDARs were isolated by switching normal ACSF to a modified zero magnesium ACSF [124 mM NaCl, 4.4 mM KCl, 3.7 mM $CaCl_2$, 1 mM NaH_2PO_4, 10 mM glucose, and 26 mM $NaHCO_3$ (pH 7.2–7.4); 290–310 mOsm] containing NBQX (10 μM) and picrotoxin (25 μM) midway through the 1.5-h incubation period. Responses were elicited at a rate of 0.0167 Hz, with an intensity of 10–20 V and a duration of 100–200 μs. Stable baselines of at least 20 min were recorded before drug application: 25 min for ethanol (100 mM), 15 min for DL-APV (100 μM), 60 min for Ro25-9681 (0.2, 2, or 10 μM), 30 min for Ro25-9681 (2 μM) in high-temperature experiments, 60 min for memantine (5 or 30 μM), 20 min for memantine (1 or 5 μM) alone and then 60 min with Ro25-6981 (2.0 μM), 30 min for ifenprodil (10 μM), and 30 min for prazosin (10 μM). Analyses were made by calculating the percent change of the N2 from baseline (averaged 10 min before drug application) to peak drug effect [ethanol: 10–19 min after drug application, DL-APV: 10–19 min after drug application, Ro25-6981: 30–39 min after drug application, memantine: 40–49 min after drug application, Ro25-6981 and memantine: early 30–39 min and late 50–59 min after drug application, Ro25-6981 (temperature): 21–30 min after drug application, ifenprodil: 30–39 min after drug application, and prazosin: 30–39 min after drug application].

Pharmacology. Ro25-6981 hydrochloride, DL-APV, NBQX hydrochloride, and memantine hydrochloride were all purchased from Ascent Scientific. Picrotoxin and ifenprodil were obtained from Tocris Bioscience. Pyrazole and prazosin were purchased from Sigma–Aldrich.

CIE. Mice were given a daily injection of either pyrazole (control group, control, 1 mmol/kg) or pyrazole + ethanol [ethanol group, ethyl alcohol (EtOH), 1 mmol/kg + 0.8 g/kg, respectively] to impair the metabolism of ethanol. Thirty minutes after the injection, in their home cages, mice were placed in a chamber filled with volatilized ethanol (EtOH, 20.3 ± 0.2 mg/L) or volatilized water (control). Airflow through the chambers was maintained at 5.5 L/min, and volatilization was maintained at 1.5 L/min. After 16 h of exposure, mice were removed from the chambers and returned to standard animal housing. Using these parameters, we can reliably obtain blood ethanol concentrations in the range of 150–185 mg/dL (80). This corresponds to a blood alcohol level of ~0.21%. For the CIE exposure paradigm, mice were given two 4-d cycles of vapor chamber exposure (16 h in chambers per day, 8 h outside chambers per day). These two cycles were separated by 3 d outside of the chambers (diagram in Fig. 5*A*).

Statistics. Analyses of Western blots; decay kinetics; sEPSCs; AMPA/NMDA ratios; and GluN2B KO LTP with and without picrotoxin, 10 μM Ro25-6981 LTP, acute ethanol in GluN2B KO, CIE LTP, and CIE with GluN2B KO experiments were conducted with unpaired *t* tests between groups. Drug applications on NMDAR fields, acute ethanol with 10 μM Ro25-6981, and Ro25-6981 effects in nonisolated fields were evaluated with paired *t* tests between drug treatments and baseline. Comparisons of PPRs between GluN2B KO and controls used two-way ANOVA. Analyses of LTP following 2.0 μM Ro25-6981/memantine and 2.0 μM Ro25-6981 in NMDR-isolated fields in CIE mice were performed with one-way ANOVA. Differences between individual groups were determined with Newman–Keuls post hoc tests.

ACKNOWLEDGMENTS. We thank Kelly Conrad and Sachin Patel for reading portions of this work and for helpful discussions. We thank Katie Louderback for artwork. The conditional GluN2B KO mouse was generated by the Integrative Neuroscience Initiative on Alcoholism (INIA)-Stress Consortium and supported by National Institutes of Health Grant U01 AA013514 (to E.D.). This work was supported by National Institutes of Health Grants AA019455 (to D.G.W.), AA019847 (to T.W.), AA020140 (to Y.S.), and MH063232 (to R.J.C.).

1. Briand LA, Vassoler FM, Pierce RC, Valentino RJ, Blendy JA (2010) Ventral tegmental afferents in stress-induced reinstatement: The role of cAMP response element-binding protein. *J Neurosci* 30:16149–16159.
2. Buffalari DM, See RE (2011) Inactivation of the bed nucleus of the stria terminalis in an animal model of relapse: Effects on conditioned cue-induced reinstatement and its enhancement by yohimbine. *Psychopharmacology (Berl)* 213:19–27.
3. Erb S, Salmaso N, Rodaros D, Stewart J (2001) A role for the CRF-containing pathway from central nucleus of the amygdala to bed nucleus of the stria terminalis in the stress-induced reinstatement of cocaine seeking in rats. *Psychopharmacology (Berl)* 158:360–365.
4. Erb S, Stewart J (1999) A role for the bed nucleus of the stria terminalis, but not the amygdala, in the effects of corticotropin-releasing factor on stress-induced reinstatement of cocaine seeking. *J Neurosci* 19:RC35.
5. Leri F, Flores J, Rodaros D, Stewart J (2002) Blockade of stress-induced but not cocaine-induced reinstatement by infusion of noradrenergic antagonists into the bed nucleus of the stria terminalis or the central nucleus of the amygdala. *J Neurosci* 22: 5713–5718.
6. Wang J, Fang Q, Liu Z, Lu L (2006) Region-specific effects of brain corticotropin-releasing factor receptor type 1 blockade on footshock-stress- or drug-priming-induced reinstatement of morphine conditioned place preference in rats. *Psychopharmacology (Berl)* 185:19–28.
7. Brigman JL, et al. (2010) Loss of GluN2B-containing NMDA receptors in CA1 hippocampus and cortex impairs long-term depression, reduces dendritic spine density, and disrupts learning. *J Neurosci* 30:4590–4600.
8. Dildy JE, Leslie SW (1989) Ethanol inhibits NMDA-induced increases in free intracellular Ca2+ in dissociated brain cells. *Brain Res* 499:383–387.
9. Hoffman PL, Rabe CS, Moses F, Tabakoff B (1989) N-methyl-D-aspartate receptors and ethanol: Inhibition of calcium flux and cyclic GMP production. *J Neurochem* 52: 1937–1940.
10. Lovinger DM, White G, Weight FF (1989) Ethanol inhibits NMDA-activated ion current in hippocampal neurons. *Science* 243:1721–1724.
11. Traynelis SF, et al. (2010) Glutamate receptor ion channels: Structure, regulation, and function. *Pharmacol Rev* 62:405–496.
12. Cull-Candy S, Brickley S, Farrant M (2001) NMDA receptor subunits: Diversity, development and disease. *Curr Opin Neurobiol* 11:327–335.
13. Dopico AM, Lovinger DM (2009) Acute alcohol action and desensitization of ligand-gated ion channels. *Pharmacol Rev* 61:98–114.
14. Hicklin TR, et al. (2011) Alcohol inhibition of the NMDA receptor function, long-term potentiation, and fear learning requires striatal-enriched protein tyrosine phosphatase. *Proc Natl Acad Sci USA* 108:6650–6655.
15. Jeanes ZM, Buske TR, Morrisett RA (2011) In vivo chronic intermittent ethanol exposure reverses the polarity of synaptic plasticity in the nucleus accumbens shell. *J Pharmacol Exp Ther* 336:155–164.
16. Ren H, Honse Y, Peoples RW (2003) A site of alcohol action in the fourth membrane-associated domain of the N-methyl-D-aspartate receptor. *J Biol Chem* 278:48815–48820.
17. Ronald KM, Mirshahi T, Woodward JJ (2001) Ethanol inhibition of N-methyl-D-aspartate receptors is reduced by site-directed mutagenesis of a transmembrane domain phenylalanine residue. *J Biol Chem* 276:44729–44735.
18. Engblom AC, Courtney MJ, Kukkonen JP, Akerman KE (1997) Ethanol specifically inhibits NMDA receptors with affinity for ifenprodil in the low micromolar range in cultured cerebellar granule cells. *J Neurochem* 69:2162–2168.
19. Fink K, Göthert M (1996) Both ethanol and ifenprodil inhibit NMDA-evoked release of various neurotransmitters at different, yet proportional potency: Potential relation to NMDA receptor subunit composition. *Naunyn Schmiedebergs Arch Pharmacol* 354: 312–319.
20. Izumi Y, Nagashima K, Murayama K, Zorumski CF (2005) Acute effects of ethanol on hippocampal long-term potentiation and long-term depression are mediated by different mechanisms. *Neuroscience* 136:509–517.
21. Lovinger DM (1995) Developmental decrease in ethanol inhibition of N-methyl-D-aspartate receptors in rat neocortical neurons: Relation to the actions of ifenprodil. *J Pharmacol Exp Ther* 274:164–172.
22. Popp RL, Lickteig RL, Lovinger DM (1999) Factors that enhance ethanol inhibition of N-methyl-D-aspartate receptors in cerebellar granule cells. *J Pharmacol Exp Ther* 289: 1564–1574.
23. Suvarna N, et al. (2005) Ethanol alters trafficking and functional N-methyl-D-aspartate receptor NR2 subunit ratio via H-Ras. *J Biol Chem* 280:31450–31459.
24. Kash TL, Matthews RT, Winder DG (2008) Alcohol inhibits NR2B-containing NMDA receptors in the ventral bed nucleus of the stria terminalis. *Neuropsychopharmacology* 33:1379–1390.
25. Weitlauf C, Egli RE, Grueter BA, Winder DG (2004) High-frequency stimulation induces ethanol-sensitive long-term potentiation at glutamatergic synapses in the dorsolateral bed nucleus of the stria terminalis. *J Neurosci* 24:5741–5747.
26. Francesconi W, et al. (2009) Protracted withdrawal from alcohol and drugs of abuse impairs long-term potentiation of intrinsic excitability in the juxtacapsular bed nucleus of the stria terminalis. *J Neurosci* 29:5389–5401.
27. Kash TL, Baucum AJ 2nd, Conrad KL, Colbran RJ, Winder DG (2009) Alcohol exposure alters NMDAR function in the bed nucleus of the stria terminalis. *Neuropsychopharmacology* 34: 2420–2429.

28. Follesa P, Ticku MK (1996) NMDA receptor upregulation: Molecular studies in cultured mouse cortical neurons after chronic antagonist exposure. *J Neurosci* 16: 2172–2178.
29. Kalluri HS, Mehta AK, Ticku MK (1998) Up-regulation of NMDA receptor subunits in rat brain following chronic ethanol treatment. *Brain Res Mol Brain Res* 58:221–224.
30. Kumari M (2001) Differential effects of chronic ethanol treatment on N-methyl-D-aspartate R1 splice variants in fetal cortical neurons. *J Biol Chem* 276:29764–29771.
31. Nagy J, Kolok S, Dezso P, Boros A, Szombathelyi Z (2003) Differential alterations in the expression of NMDA receptor subunits following chronic ethanol treatment in primary cultures of rat cortical and hippocampal neurones. *Neurochem Int* 42:35–43.
32. Pawlak R, Melchor JP, Matys T, Skrzypiec AE, Strickland S (2005) Ethanol-withdrawal seizures are controlled by tissue plasminogen activator via modulation of NR2B-containing NMDA receptors. *Proc Natl Acad Sci USA* 102:443–448.
33. Sheela Rani CS, Ticku MK (2006) Comparison of chronic ethanol and chronic intermittent ethanol treatments on the expression of GABA(A) and NMDA receptor subunits. *Alcohol* 38:89–97.
34. Carpenter-Hyland EP, Woodward JJ, Chandler LJ (2004) Chronic ethanol induces synaptic but not extrasynaptic targeting of NMDA receptors. *J Neurosci* 24: 7859–7868.
35. Clapp P, Gibson ES, Dell'acqua ML, Hoffman PL (2010) Phosphorylation regulates removal of synaptic N-methyl-D-aspartate receptors after withdrawal from chronic ethanol exposure. *J Pharmacol Exp Ther* 332:720–729.
36. Kash T, Winder D (2007) NMDAR LTP and LTD induction: 2B or not 2B…is that the question? *Debates Neurosci* 1:79–84.
37. Keiser MJ, et al. (2009) Predicting new molecular targets for known drugs. *Nature* 462:175–181.
38. Paoletti P, Neyton J (2007) NMDA receptor subunits: Function and pharmacology. *Curr Opin Pharmacol* 7:39–47.
39. Weitlauf C, et al. (2005) Activation of NR2A-containing NMDA receptors is not obligatory for NMDA receptor-dependent long-term potentiation. *J Neurosci* 25: 8386–8390.
40. Kutsuwada T, et al. (1996) Impairment of suckling response, trigeminal neuronal pattern formation, and hippocampal LTD in NMDA receptor epsilon 2 subunit mutant mice. *Neuron* 16:333–344.
41. Badanich KA, et al. (2011) NR2B deficient mice are more sensitive to the locomotor stimulant and depressant effects of ethanol. *Genes Brain Behav* 10:805–816.
42. von Engelhardt J, et al. (2008) Contribution of hippocampal and extra-hippocampal NR2B-containing NMDA receptors to performance on spatial learning tasks. *Neuron* 60:846–860.
43. Fischer G, et al. (1997) Ro 25-6981, a highly potent and selective blocker of N-methyl-D-aspartate receptors containing the NR2B subunit. Characterization in vitro. *J Pharmacol Exp Ther* 283:1285–1292.
44. Kew JN, Trube G, Kemp JA (1996) A novel mechanism of activity-dependent NMDA receptor antagonism describes the effect of ifenprodil in rat cultured cortical neurones. *J Physiol* 497:761–772.
45. Zhang XX, Bunney BS, Shi WX (2000) Enhancement of NMDA-induced current by the putative NR2B selective antagonist ifenprodil. *Synapse* 37:56–63.
46. Zhang XX, Shi WX (2001) Dynamic modulation of NMDA-induced responses by ifenprodil in rat prefrontal cortex. *Synapse* 39:313–318.
47. Milnerwood AJ, et al. (2010) Early increase in extrasynaptic NMDA receptor signaling and expression contributes to phenotype onset in Huntington's disease mice. *Neuron* 65:178–190.
48. Bordji K, Becerril-Ortega J, Nicole O, Buisson A (2010) Activation of extrasynaptic, but not synaptic, NMDA receptors modifies amyloid precursor protein expression pattern and increases amyloid-β production. *J Neurosci* 30:15927–15942.
49. Léveillé F, et al. (2008) Neuronal viability is controlled by a functional relation between synaptic and extrasynaptic NMDA receptors. *FASEB J* 22:4258–4271.
50. Okamoto S, et al. (2009) Balance between synaptic versus extrasynaptic NMDA receptor activity influences inclusions and neurotoxicity of mutant huntingtin. *Nat Med* 15:1407–1413.
51. Xia P, Chen HS, Zhang D, Lipton SA (2010) Memantine preferentially blocks extrasynaptic over synaptic NMDA receptor currents in hippocampal autapses. *J Neurosci* 30:11246–11250.
52. Asztely F, Erdemli G, Kullmann DM (1997) Extrasynaptic glutamate spillover in the hippocampus: Dependence on temperature and the role of active glutamate uptake. *Neuron* 18:281–293.
53. Wadiche JI, Kavanaugh MP (1998) Macroscopic and microscopic properties of a cloned glutamate transporter/chloride channel. *J Neurosci* 18:7650–7661.
54. Leonard AS, Lim IA, Hemsworth DE, Horne MC, Hell JW (1999) Calcium/calmodulin-dependent protein kinase II is associated with the N-methyl-D-aspartate receptor. *Proc Natl Acad Sci USA* 96:3239–3244.
55. Strack S, Colbran RJ (1998) Autophosphorylation-dependent targeting of calcium/calmodulin-dependent protein kinase II by the NR2B subunit of the N-methyl-D-aspartate receptor. *J Biol Chem* 273:20689–20692.
56. Strack S, McNeill RB, Colbran RJ (2000) Mechanism and regulation of calcium/calmodulin-dependent protein kinase II targeting to the NR2B subunit of the N-methyl-D-aspartate receptor. *J Biol Chem* 275:23798–23806.
57. Akashi K, et al. (2009) NMDA receptor GluN2B (GluR epsilon 2/NR2B) subunit is crucial for channel function, postsynaptic macromolecular organization, and actin cytoskeleton at hippocampal CA3 synapses. *J Neurosci* 29:10869–10882.
58. Barria A, Malinow R (2005) NMDA receptor subunit composition controls synaptic plasticity by regulating binding to CaMKII. *Neuron* 48:289–301.
59. Bartlett TE, et al. (2007) Differential roles of NR2A and NR2B-containing NMDA receptors in LTP and LTD in the CA1 region of two-week old rat hippocampus. *Neuropharmacology* 52:60–70.
60. de Marchena J, et al. (2008) NMDA receptor antagonists reveal age-dependent differences in the properties of visual cortical plasticity. *J Neurophysiol* 100: 1936–1948.
61. Chen Q, et al. (2007) Differential roles of NR2A- and NR2B-containing NMDA receptors in activity-dependent brain-derived neurotrophic factor gene regulation and limbic epileptogenesis. *J Neurosci* 27:542–552.
62. Fox CJ, Russell KI, Wang YT, Christie BR (2006) Contribution of NR2A and NR2B NMDA subunits to bidirectional synaptic plasticity in the hippocampus in vivo. *Hippocampus* 16:907–915.
63. Izumi Y, Auberson YP, Zorumski CF (2006) Zinc modulates bidirectional hippocampal plasticity by effects on NMDA receptors. *J Neurosci* 26:7181–7188.
64. Liu L, et al. (2004) Role of NMDA receptor subtypes in governing the direction of hippocampal synaptic plasticity. *Science* 304:1021–1024.
65. Massey PV, et al. (2004) Differential roles of NR2A and NR2B-containing NMDA receptors in cortical long-term potentiation and long-term depression. *J Neurosci* 24: 7821–7828.
66. Wu PH, Coultrap SJ, Browning MD, Proctor WR (2011) Functional adaptation of the N-methyl-D-aspartate receptor to inhibition by ethanol is modulated by striatal-enriched protein tyrosine phosphatase and p38 mitogen-activated protein kinase. *Mol Pharmacol* 80:529–537.
67. Anders DL, Blevins T, Sutton G, Chandler LJ, Woodward JJ (1999) Effects of c-Src tyrosine kinase on ethanol sensitivity of recombinant NMDA receptors expressed in HEK 293 cells. *Alcohol Clin Exp Res* 23:357–362.
68. Blevins T, Mirshahi T, Chandler LJ, Woodward JJ (1997) Effects of acute and chronic ethanol exposure on heteromeric N-methyl-D-aspartate receptors expressed in HEK 293 cells. *J Neurochem* 69:2345–2354.
69. Chu B, Anantharam V, Treistman SN (1995) Ethanol inhibition of recombinant heteromeric NMDA channels in the presence and absence of modulators. *J Neurochem* 65:140–148.
70. Jin C, Woodward JJ (2006) Effects of 8 different NR1 splice variants on the ethanol inhibition of recombinant NMDA receptors. *Alcohol Clin Exp Res* 30:673–679.
71. Hendricson AW, et al. (2007) Aberrant synaptic activation of N-methyl-D-aspartate receptors underlies ethanol withdrawal hyperexcitability. *J Pharmacol Exp Ther* 321: 60–72.
72. Thomas MP, Monaghan DT, Morrisett RA (1998) Evidence for a causative role of N-methyl-D-aspartate receptors in an in vitro model of alcohol withdrawal hyperexcitability. *J Pharmacol Exp Ther* 287:87–97.
73. Philpot BD, Cho KK, Bear MF (2007) Obligatory role of NR2A for metaplasticity in visual cortex. *Neuron* 53:495–502.
74. Conrad KL, Louderback KM, Gessner CP, Winder DG (2011) Stress-induced alterations in anxiety-like behavior and adaptations in plasticity in the bed nucleus of the stria terminalis. *Physiol Behav* 104:248–256.
75. Roberto M, et al. (2004) Acute and chronic ethanol alter glutamatergic transmission in rat central amygdala: an in vitro and in vivo analysis. *J Neurosci* 24:1594–1603.
76. Roberto M, Bajo M, Crawford E, Madamba SG, Siggins GR (2006) Chronic ethanol exposure and protracted abstinence alter NMDA receptors in central amygdala. *Neuropsychopharmacology* 31:988–996.
77. Gladding CM, Raymond LA (2011) Mechanisms underlying NMDA receptor synaptic/extrasynaptic distribution and function. *Mol Cell Neurosci* 48:308–320.
78. Hardingham GE, Bading H (2010) Synaptic versus extrasynaptic NMDA receptor signalling: Implications for neurodegenerative disorders. *Nat Rev Neurosci* 11: 682–696.
79. Krupitsky EM, et al. (2007) Effect of memantine on cue-induced alcohol craving in recovering alcohol-dependent patients. *Am J Psychiatry* 164:519–523.
80. McNeill RB, Colbran RJ (1995) Interaction of autophosphorylated Ca2+/calmodulin-dependent protein kinase II with neuronal cytoskeletal proteins. Characterization of binding to a 190-kDa postsynaptic density protein. *J Bio Chem* 270:10043–10049.
81. Healey JC, Winder DG, Kash TL (2008) Chronic ethanol exposure leads to divergent control of dopaminergic synapses in distinct target regions. *Alcohol* 42:179–190.